Technical Note: Use of the OPS software for local processing and comparison with global IASI data

Philippe Marguinaud (Météo-France)
Pascal Brunel (Météo-France)

Change record			
Version	Date	Author / changed by	Remarks
1.0	September 21, 2007	Philippe Marguinaud Pascal Brunel	First release

Contents

1 Introduction **3**

2 Global and local preprocessing **3**
2.1 Differences between the nominal OPS and the OPS-LRS packages 3
2.2 Specific issues of local preprocessing 3

3 Test data set provided by CNES **3**

4 Comparison of OPS and OPS-LRS used for global processing **5**

5 Comparison of global processing and local processing with OPS-LRS **5**
5.1 Influence of the empty context 5
5.2 Influence of the interferometer axis position history 6
5.3 Influence of the black body temperature history 7

6 Direct comparison of local and global IASI 1C data **7**

7 Validation of OPS_V3-6 + patches 2, 3, 4, 5, 6, 7, 8, 9 **8**

8 Conclusion **9**

1 Introduction

The OPS software for IASI level 0 preprocessing has been modified for local processing and is distributed by the NWP-SAF as OPS-LRS with the ATOVS and AVHRR preprocessing package AAPP.

The OPS-LRS is now used in routine at Lannion (Météo-France/CMS) and at Exeter (UKMO) to process level 0 data from local reception. The level 1C spectra produced in Lannion are sent to Toulouse and inserted in the operational observations database to be assimilated by NWP forecast models in the future.

On the other hand, global IASI data pre-processing takes place at Eumetsat. The spectra produced there are distributed later (at least one hour) because of the time constraints on data processing.

The question of the compatibility of these two sources of IASI level 1C spectra has to be examined; this is the purpose of this document.

2 Global and local preprocessing

2.1 Differences between the nominal OPS and the OPS-LRS packages

The OPS software integrates two proprietary components which have been replaced in OPS-LRS.

- The MetopLib navigation library; this has been replaced by the AAPP navigation libraries.
- The IBM scientific library ESSL; pieces of software pulled from public domain libraries have been used (fftw3, ngmath, lapack, cubic spline implementation from numerical recipies).

Other modifications have been applied to the original OPS, but these are for portability purposes only and should not affect the scientific algorithms.

2.2 Specific issues of local preprocessing

The nominal OPS software makes use of a context file, which contains all the important historic data the preprocessing requires. This context file is saved before the software stops and re-used when the software re-starts. Having time series of on-board measured data helps eliminating the measurement noise.

But in the case of local reception, it is not possible to start but with an empty context, because the processor is not fed with a continuous stream of data. Using a context from the last processing would not make sense and would provide spurious data to the processor. Therefore there is no other choice but to use an empty context, and this implies that the spectra produced from a local reception will be different from those of the global 1C stream.

3 Test data set provided by CNES

The CNES has provided us with a full orbit test case, processed with the OPS_V3-6 + patchs 2, 3, 4, 5, 6. The following input files were provided:

```
aux_data/IASI_CTX_xx_M02_20070402163553Z_xxxxxxxxxxxxxxx_20070403224317Z_CGS1_xxxxx02343
aux_data/IASI_GRD_xx_M02_20070329120000Z_xxxxxxxxxxxxxxZ_20070329084411Z_IAST_0000000008
aux_data/IASI_CTX_xx_M02_20070402145353Z_xxxxxxxxxxxxxxx_20070403195723Z_CGS1_xxxxx02342
aux_data/IASI_ODB_xx_M02_20070329120000Z_xxxxxxxxxxxxxxZ_20070329083257Z_IAST_0000000004
aux_data/IASI_BRD_xx_M02_20070329120500Z_xxxxxxxxxxxxxxZ_20070329091915Z_IAST_0000000006
aux_data/AVHR_xxx_1B_M02_20070402145503Z_20070402163703Z_N_O_20070402163505Z
aux_data/AVHR_xxx_1B_M02_20070402131603Z_20070402145503Z_N_O_20070402145532Z
aux_data/xxxx_SVM_xx_M02_20070328000000Z_20070407000000Z_20070328081807Z_FDFx_FDGEOEVENT
aux_data/IASI_ODB_xx_M02_20070329120000Z_xxxxxxxxxxxxxxZ_20070329083257Z_IAST_0000000004
aux_data/IASI_BRD_xx_M02_20070329120500Z_xxxxxxxxxxxxxxZ_20070329091915Z_IAST_0000000006
aux_data/IASI_GRD_xx_M02_20070329120000Z_xxxxxxxxxxxxxxZ_20070329084411Z_IAST_0000000008
aux_data/xxxx_OBT_xx_M01_20070402145400Z_20070402163600Z_20070403212318Z_FDFx_METOOBTUTC
aux_data/IASI_CTX_xx_M02_20061221045654Z_xxxxxxxxxxxxxxx_20061221171712Z_CMSx_xxxxx00000
IASI_1_wo_001
product_model
product_model/IASI_xxx_1C_M02_xxxxxxxxxxxxxxZ_xxxxxxxxxxxxxxZ_V_T_xxxxxxxxxxxxxxZ
product_model/IASI_xxx_1A_M02_xxxxxxxxxxxxxxZ_xxxxxxxxxxxxxxZ_V_T_xxxxxxxxxxxxxxZ
product_model/IASI_ENG_01_M02_xxxxxxxxxxxxxxZ_xxxxxxxxxxxxxxZ_V_T_xxxxxxxxxxxxxxZ
product_model/IASI_xxx_1B_M02_xxxxxxxxxxxxxxZ_xxxxxxxxxxxxxxZ_V_T_xxxxxxxxxxxxxxZ
product_model/IASI_VER_01_M02_xxxxxxxxxxxxxxZ_xxxxxxxxxxxxxxZ_V_T_xxxxxxxxxxxxxxZ
unproc_data
unproc_data/IASI_xxx_00_M02_20070402145400Z_20070402163600Z_N_O_20070402162953Z
```

And verification data was provided too:

```
IASI_ENG_01_M02_20070402145401Z_20070402150353Z_V_T_20070404084828Z
SD.log
IASI_xxx_1B_M02_20070402145401Z_20070402150353Z_V_T_20070404084827Z
IASI_VER_01_M02_20070402145401Z_20070402150353Z_V_T_20070404084828Z
IASI_CTX_xx_M02_20070402150353Z_xxxxxxxxxxxxxxx_20070404091535Z_CGS1_xxxxx02343
IASI_1_wo_001_001.rpt
IASI_xxx_1C_M02_20070402145401Z_20070402150353Z_V_T_20070404084827Z
IASI_xxx_1A_M02_20070402145401Z_20070402150353Z_V_T_20070404084827Z
```

The work-order is detailed below:

```
<?xml version="1.0" encoding="UTF-8"?>
<!DOCTYPE PPF_Work_Order SYSTEM "PPF_Work_Order.dtd">
<PPF_Work_Order>
<ProcessingType>L1a</ProcessingType>
<SensingStart>20070402145400Z</SensingStart>
<SensingStop>20070402150400Z</SensingStop>
<TimeIntervalFlag>Full</TimeIntervalFlag>
<TimeIntervalCounter>1</TimeIntervalCounter>
<UnProcData>input/unproc_data/IASI_xxx_00_M02_20070402145400Z_20070402163600Z_N_O_20070402162953Z</UnProcData>
<AuxData>input/aux_data/AVHR_xxx_1B_M02_20070402131603Z_20070402145503Z_N_O_20070402145532Z</AuxData>
<AuxData>input/aux_data/AVHR_xxx_1B_M02_20070402145503Z_20070402163703Z_N_O_20070402163505Z</AuxData>
<AuxData>input/aux_data/xxxx_SVM_xx_M02_20070328000000Z_20070407000000Z_20070328081807Z_FDFx_FDGEOEVENT</AuxData>
<AuxData>input/aux_data/xxxx_OBT_xx_M01_20070402145400Z_20070402163600Z_20070403212318Z_FDFx_METOOBTUTC</AuxData>
<AuxData>input/aux_data/IASI_BRD_xx_M02_20070329120500Z_xxxxxxxxxxxxxxZ_20070329091915Z_IAST_0000000006</AuxData>
<AuxData>input/aux_data/IASI_GRD_xx_M02_20070329120000Z_xxxxxxxxxxxxxxZ_20070329084411Z_IAST_0000000008</AuxData>
<AuxData>input/aux_data/IASI_ODB_xx_M02_20070329120000Z_xxxxxxxxxxxxxxZ_20070329083257Z_IAST_0000000004</AuxData>
<AuxData>input/aux_data/IASI_CTX_xx_M02_20070402145353Z_xxxxxxxxxxxxxxx_20070403195723Z_CGS1_xxxxx02342</AuxData>
<ProdModel>input/product_model/IASI_xxx_1A_M02_xxxxxxxxxxxxxxZ_xxxxxxxxxxxxxxZ_V_T_xxxxxxxxxxxxxxZ</ProdModel>
<ProdModel>input/product_model/IASI_xxx_1B_M02_xxxxxxxxxxxxxxZ_xxxxxxxxxxxxxxZ_V_T_xxxxxxxxxxxxxxZ</ProdModel>
<ProdModel>input/product_model/IASI_xxx_1C_M02_xxxxxxxxxxxxxxZ_xxxxxxxxxxxxxxZ_V_T_xxxxxxxxxxxxxxZ</ProdModel>
<ProdModel>input/product_model/IASI_ENG_01_M02_xxxxxxxxxxxxxxZ_xxxxxxxxxxxxxxZ_V_T_xxxxxxxxxxxxxxZ</ProdModel>
<ProdModel>input/product_model/IASI_VER_01_M02_xxxxxxxxxxxxxxZ_xxxxxxxxxxxxxxZ_V_T_xxxxxxxxxxxxxxZ</ProdModel>
</PPF_Work_Order>
```

Note that the test case is supplied with a work-order which specifies to process only the first ten minutes of data.

It turns out that although the context file marked with the orbit number 2342 was specified, the OPS software has the ability to pick the context file 2343 which is present in the auxiliary data directory. And here, this is what it did.

At least, this is what we suppose, since results with the OPS-LRS starting from context 2343 are very close to the CNES reference, while results starting from context 2342 (obtained by removing the context 2343) exhibits very strong differences. This has been confirmed later by running the original OPS on IBM AIX.

Comparisons with CNES reference are therefore based on OPS-LRS working with the context 2343; as a comparison of the two packages with the same input data, this seem to be acceptable.

4 Comparison of OPS and OPS-LRS used for global processing

We start with context 2343 on the CNES test case.

After discussions with the CNES and investigations, it appeared that the choice of the cubic spline interpolator which is used for resampling IASI spectra has a strong influence on the results. We have tried several spline interpolators and discussions with the CNES helped us to choose the spline interpolator which gives the best results (cubic spline with free ends conditions).

Figure 1 shows the bias, quadratic error, and maximum positive and negative differences (red and blue dots); these differences are very small, around $0.02K$ for largest values below $2200cm^{-1}$ and around $0.2K$ at $2500cm^{-1}$, where the instrument noise is quite large (see figure 7). These are the differences of the first ten minutes of processing only.

The conclusion is that the results yielded by OPS and OPS-LRS are very close to each other.

5 Comparison of global processing and local processing with OPS-LRS

5.1 Influence of the empty context

Having proved that OPS-LRS reproduces very well the results of OPS when provided with the same data, we can use it to simulate global processing. We have processed the full orbit 2343 starting from **context 2342**; this provided a reference similar to what we get from Eumetsat IASI level 1C broadcast.

The orbit 2343 has also been processed using an **empty context** file; this corresponds to what is done at CMS and UKMO.

We recall here that, for each wavenumber ν :

$$NeDT_{280K}(\Delta R(\nu)) = \frac{\Delta R(\nu)}{(\partial B(T,\nu)/\partial T)_{T=280K}}$$

Where:

- $\Delta R(\nu)$ is the radiance difference.

- $B(T, \nu)$ is the Planck function.

This is the measure we use to compare with the expected instrument noise.

The figures 2 and 3 show the percentage of IASI radiances where $NeDT_{280K}(difference) < 0.1 * NeDT_{280K}(instrument)$ for each IASI scan line. We have also represented the longitude, latitude and the exposure of satellite to sunlight (0 means day and 1 is night). The comparison between these two series of IASI data shows that level 1A spectra converge very quickly (figure 2), but this is not the case for 1C data (figure 3). The differences observed on IASI 1C data seem to be influenced by the position of the satellite (differences stronger when close to the equator) and by its exposure to sunlight.

For this test case the maximum of $NeDT_{280K}(difference)/NeDT_{280K}(instrument)$ for level 1C is always less than 1. (figure 4). Figure 4 shows that the NeDT ratio is always roughly a multiple of 0.2; the explanation lies in the scaling factors used to encode the radiances in level 1C files and in the instrument noise: figure 6 shows the difference observed in terms of NeDT for a difference in numerical counts of a unit. When divided by the instrument noise (figure 7), this curve yields figure 8, whose peak is at $(1250cm^{-1}, 0.2)$. There is also a wavenumber range $[1200cm^{-1}..1450cm^{-1}]$ where $NeDT(1nc)/NeDT(inst)$ is large; extreme values for $NeDT(\Delta R)/NeDT(inst)$ are always observed in this wavenumber range. It should be emphasized that the noise curve and the scaling factor curve although they look similar, have uncorrelated extrema and this is the reason of the large peaks we observe in figure 8.

Figure 5 is identical to 4 except that differences have been computed using non-discretized spectra in double precision (which are not a standard output of OPS-LRS, we had to modify the software for that purpose); we also show the corresponding brightness temperatures and wavenumbers. Figure 9 shows statistics of differences for the non-discretized spectra, ranked by wavenumbers; we clearly see that although on average these differences are not very important (less than $0.07 * NeDT$ at $1250cm^{-1}$, central plot), they can be ten times larger (upper plot).

Figures 10 and 11 show differences over the IASI spectrum for two periods of 15 minutes extracted from the full orbit; the first period starts 30 minutes after the start of the processing and lasts 15 minutes, the second period is the last 15 minutes of the orbit.

The shape of these diagrams is to be compared with figure 6, and is an effect of the discret storage of IASI radiances.

5.2 Influence of the interferometer axis position history

In the previous subsection, we have proven that the differences between local and global processing are explained by the use of an empty context in the case of local processing.

Observing that the local level 1A converge very quickly to global level 1A while convergence of level 1C takes a very long time, we foresee that the cause of this slow convergence is the empty historical data of interferometer axis position used in local processing.

Figure 12 shows the difference of position of interferometer axis of level 1C data produced starting with an empty context and level 1C data starting using the context 2342; that is, the quantity:

$$\sqrt{(GFaxAxeY_{2342}(t) - GFaxAxeY_0(t))^2 + (GFaxAxeZ_{2342}(t) - GFaxAxeZ_0(t))^2}$$

We observe that this quantity seems to converge similarly to level 1C, that is, it takes a full orbit to have very small differences.

Figures 14 and 13 show the positions of the interferometric axis for runs starting from an empty context and context 2342. We observe the following points:

- Non-filtered axis positions are very noisy (when compared to the smoothed, averaged position); the noise is maximum over the cold pole (South pole on figures 14 and 13).
- Non-filtered axis positions are identical (figures are in fact equal up to machine precision).
- Filtered axis positions are different; we observe that the axis position curve is quite flat for the run starting from 2342, while it takes some time to adapt for the run starting from an empty context.

We have carried out another run with a custom context to validate our assumption that the empty interferometer axis position history is the cause of the differences we observe between level 1C data based on an empty context and 1C data based on initialised context.

For this purpose, we created a context with empty and uninitialized data but interferometer axis position, that we copied from context 2342.

Figure 15 shows a dramatic reduction of the differences observed in figure 3; this confirms that the non-initialized interferometer axis position history is responsible of the differences we observe between local and global processing. Figure 15 appears to be very similar to figure 2 which probably means that most of the differences in the processing between level 1A and level 1C have been eliminated by filling in the appropriate interferometer axis position.

Looking at figure 12 suggest that using a constant (averaged) position of the interferometer axis would help, but it is not the case: Figure 20 shows the evolution of the context axis (Y-position and Z-position); we observe that the variation of the intra-day axis position is about the same as the correction we need to apply. That is, we cannot use a constant (say, averaged over a day or half a day) interferometer axis, to be consistent with global processing.

5.3 Influence of the black body temperature history

We have also looked at the differences of black body temperature between runs based on an empty context and on context 2342 (figure 16); these differences are very small (around $0.001K$). The time scale observed to reach very small differences is about the same as for level 1A convergence. This is because black body temperature varies very smoothly and quite predictably (see figure 19, which shows the intra-day evolution of black body temperature).

It seems that most of level 1A differences can be explained with black body temperature history; we have confirmed that by creating a custom context where only the black body temperature history is initialized and starting the OPS with this context.

6 Direct comparison of local and global IASI 1C data

Figures 17 and 18 show the differences observed for a morning case and an evening case.

Differences appear to be slightly larger for evening data; note that brightness temperature differences around $3.9\mu m$ are large, but are actually observed for low brightness temperatures, which dramatically reduces their significance.

We have also observed many cases where $NeDT(\Delta R) > NeDT(inst)$, all of them being located in the critical wavenumber range $[1200cm^{-1}..1450cm^{-1}]$.

Geolocation and datation are monitored too, and very close to each other (errors less than $100m$ at nadir, $1.2km$ at edge of scan and less than $100ms$).

Degraded cases are always identical for both Eumetsat and local 1C data.

7 Validation of OPS_V3-6 + patches 2, 3, 4, 5, 6, 7, 8, 9

On the 14/09, CNES has provided us with a new test data set (full 100 minutes orbit 3704, 07/07/2007). We have validated PS_V3-6 + patches 2, 3, 4, 5, 6, 7, 8, 9 against this test case, starting from the provided initialized context and got very good results; the full orbit pasted more than 700 IASI lines, and below are statistics computed over 200 of these lines:

```
Titre  differences fichiers iasi 1c en Tb
nombre de classes   17
valeurs initiales   202860936
valeurs conservées  202860936
min       -0.014218970384035856
max       0.010158436686594996
moyenne   -2.0016341132532822E-11
stdev     1.2269195115630816E-6
rms       1.2269195117263415E-6

histogramme :
                        nvals     cumul  pourcent
[    inf   -10.000[         0
[ -10.000,  -5.000[         0   0.00000    0.0000
[  -5.000,  -1.000[         0   0.00000    0.0000
[  -1.000,  -0.500[         0   0.00000    0.0000
[  -0.500,  -0.300[         0   0.00000    0.0000
[  -0.300,  -0.200[         0   0.00000    0.0000
[  -0.200,  -0.100[         0   0.00000    0.0000
[  -0.100,  -0.050[         0   0.00000    0.0000
[  -0.050,  -0.025[         0   0.00000    0.0000
[  -0.025,   0.025[ 202860936   1.00000  100.0000
[   0.025,   0.050[         0   1.00000    0.0000
[   0.050,   0.100[         0   1.00000    0.0000
[   0.100,   0.200[         0   1.00000    0.0000
[   0.200,   0.300[         0   1.00000    0.0000
[   0.300,   0.500[         0   1.00000    0.0000
[   0.500,   1.000[         0   1.00000    0.0000
[   1.000,   5.000[         0   1.00000    0.0000
[   5.000,  10.000[         0   1.00000    0.0000
[    sup    10.000[         0
[ bad qual flag 1 [        24
[ bad qual flag 2 [        24
```

The brightness temperature differences are about $1.22 \times 10^{-6}K$ on average and $0.014K$ at most, which is better than what we got with the previous version of OPS. This suggests that the test case provided for OPS_V3-6 + patches 2, 3, 4, 5, 6 was produced using a version of the OPS *close* to OPS_V3-6 + patches 2, 3, 4, 5, 6, but slightly different.

Unfortunately, it was not possible to compare our results with Eumetsat, because they did not use this software version on the 7th of July.

This OPS-LRS version will be delivered to NWP SAF by the end of September 2007.

8 Conclusion

We have proved that when provided with identical data, OPS and OPS-LRS give identical results (when provided with the same input data).

The OPS-LRS results on test case 2343, started from a real initialized context or from an empty context show that the differences observed between local and global level 1C radiances are explained by the different context files used at Eumetsat and at CMS.

It is also clear that the context file parameter of importance to explain these differences is the interferometer axis position historical data.

Let us recall that operational conditions for local reception are similar to start of processing with an empty context file, that is, with empty historical data for parameters such as interferometer axis position, black body temperature, etc ...

We have also observed that strongest differences occur where the radiances are the highest: near the equator, during daytime. Some questions arise:

- Obviously the question of whether these radiances are acceptable for NWP models arise. This question can only be answered by comparing retrievals of atmospheric variables from local and global IASI data.
- Is it possible to lessen the differences between local and global processing, by choosing some adequate context axis position values ? Looking at time series of context axis position (from global processing) suggests that this parameter behaves randomly enough to be unpredictable.
- Would it be acceptable for global processing to use a constant (updated on a regular basis) value for the interferometer axis position ? From the discussions we had with the CNES, we have understood that the axis position variations are very tiny. This would settle the issue of the small discrepancies observed between local and global processing.

List of Figures

1 Differences of brightness temperatures between OPS and OPS-LRS starting from context 2343 (first 10 minutes of processing) . . . 11
2 Comparison of IASI 1A spectra between local and global processing; number of cases where $NeDT(\Delta R) < 0.1 \times NeDT(inst)$; longitude; latitude; exposure to sun. X axis is second of the day. . . . 12
3 Comparison of IASI 1C spectra between local and global processing; number of cases where $NeDT(\Delta R) < 0.1 \times NeDT(inst)$; longitude; latitude; exposure to sun. X axis is second of the day. . . . 13
4 Maximum of $NeDT(\Delta R)/NeDT(inst)$ 1C spectra; for each scan line the maximum value is chosen, regardless of its wavenumber . . . 14
5 Maximum of $NeDT(\Delta R)/NeDT(inst)$ (non-discretized 1C spectra, double precision); associated brightness temperature; associated wavenumber. . . . 15
6 Variation of NeDT for a unit variation in numerical counts; with 1c scaling factors as of May 2007 . . . 16
7 NeDT of IASI instrument; as provided by D. Blumstein (ISSWG18), NeDT IPR2 FM2 full resolution as of 30/11/2005 . . . 17
8 NeDT/NeDT(instr) for a unit variation in numerical counts . . . 18
9 Maximum of NeDT(difference)/NeDT(instrument) (non-discretized spectra) . . . 19
10 Brightness temperatures differences from time 55800 to 56700, orbit 2343, 15 minute period starting 30 minutes after start of processing . . . 20
11 Brightness temperatures differences from time 57900 to 58800, orbit 2343, 15 minute period starting 70 minutes after start of processing . . . 21
12 Difference (degrees) of filtered interferometer axis position, empty context, context 2342 22
13 Position of interferometer axis position, instantaneous and filtered, starting from context 2342, GIaxAxeY, GFaxAxeY, GIaxAxeZ, GFaxAxeZ . . . 23
14 Position of interferometer axis position, instantaneous and filtered, starting from an empty context, GIaxAxeY, GFaxAxeY, GIaxAxeZ, GFaxAxeZ . . . 24
15 Comparison of IASI 1C spectra between global and local processing (non-empty axis position history) . . . 25
16 Difference of black body temperatures between runs based on empty context and context 2342 . . . 26
17 Differences of brightness temperatures between local and global processing 09:23 10/06/2007 27
18 Differences of brightness temperatures between local and global processing 22:31 10/06/2007 28
19 Variation of black body temperature over a one-day period 2007/06/03 (from L. Fiedler) 29
20 Evolution of interferometer axis position over a one-day period 2007/06/03 (from L. Fiedler) . . . 30

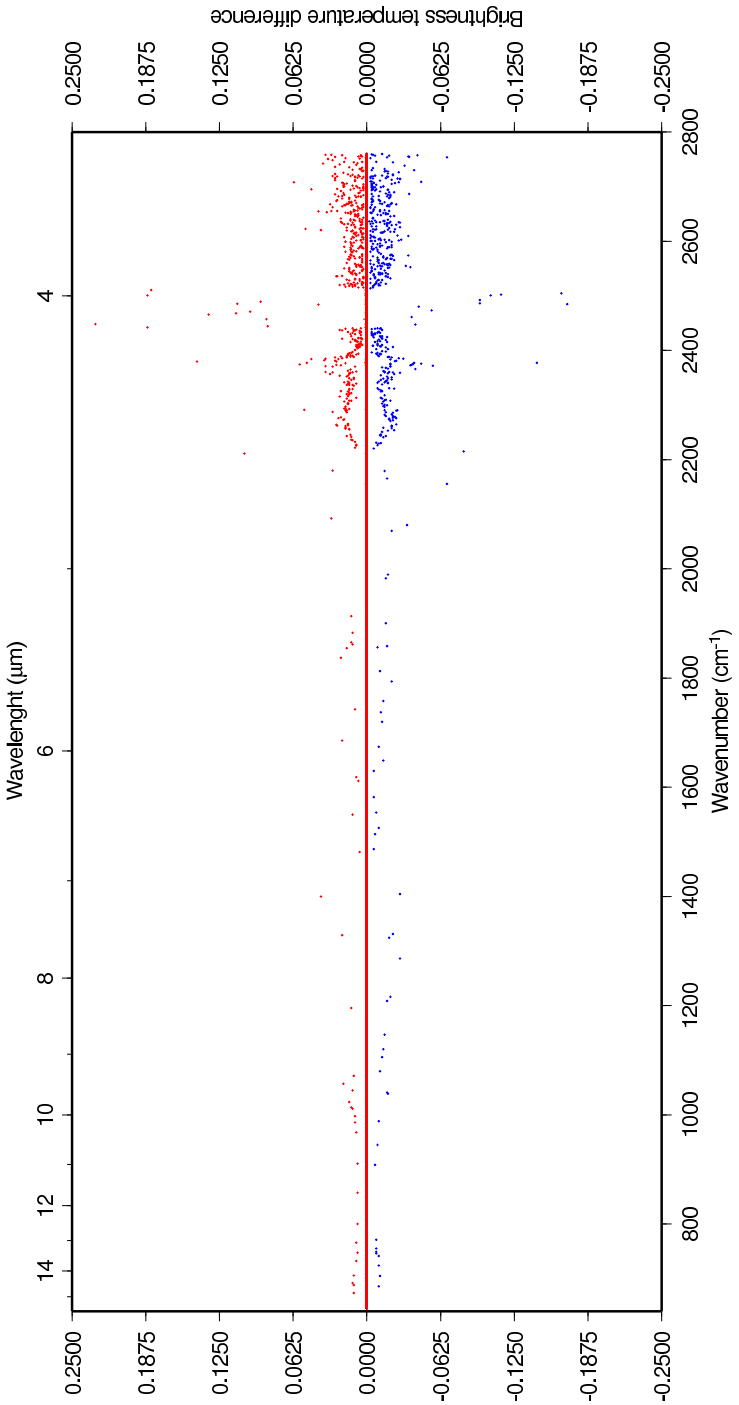

Figure 1: Differences of brightness temperatures between OPS and OPS-LRS starting from context 2343 (first 10 minutes of processing)

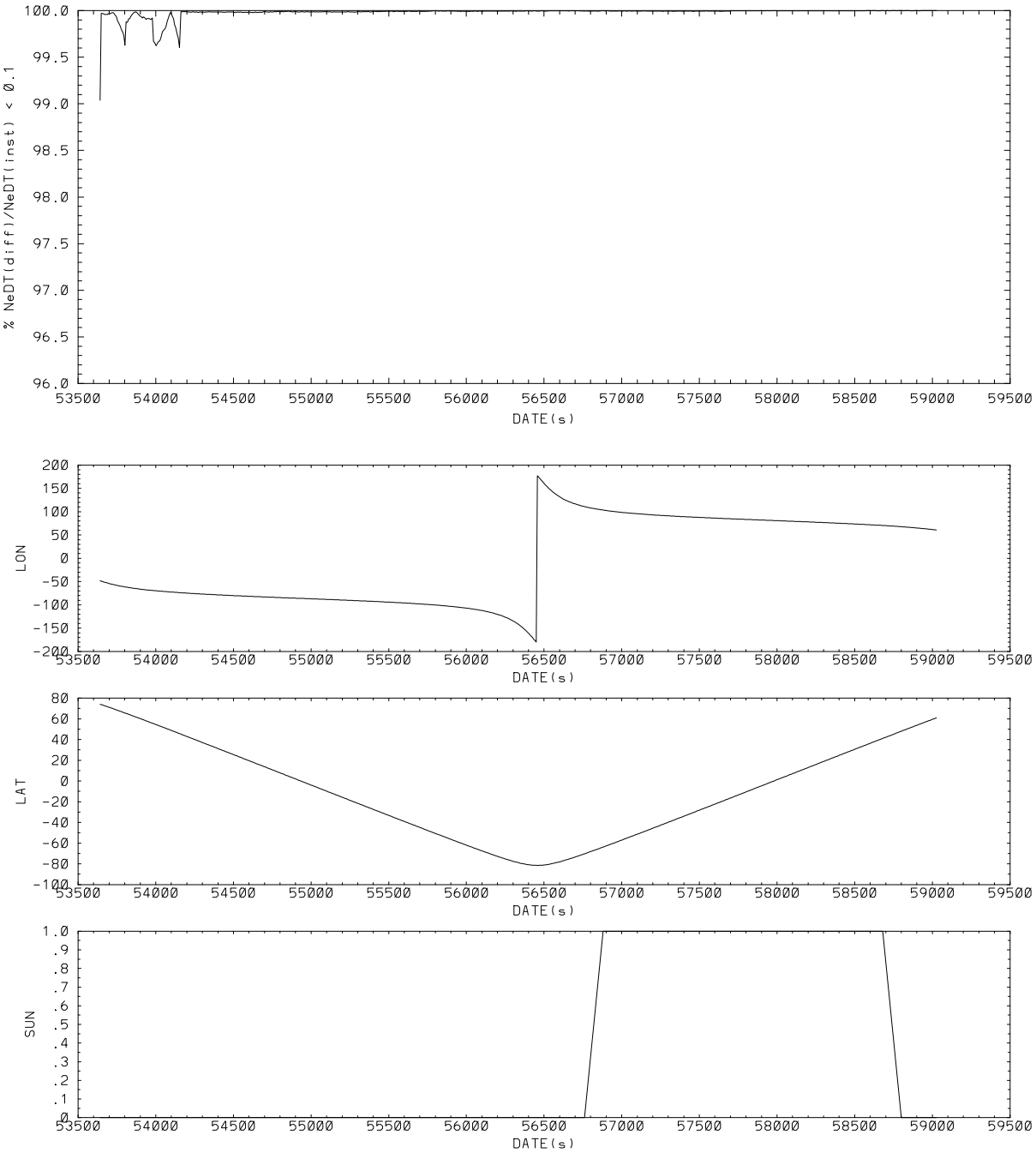

Figure 2: Comparison of IASI 1A spectra between local and global processing; number of cases where $NeDT(\Delta R) < 0.1 \times NeDT(inst)$; longitude; latitude; exposure to sun. X axis is second of the day.

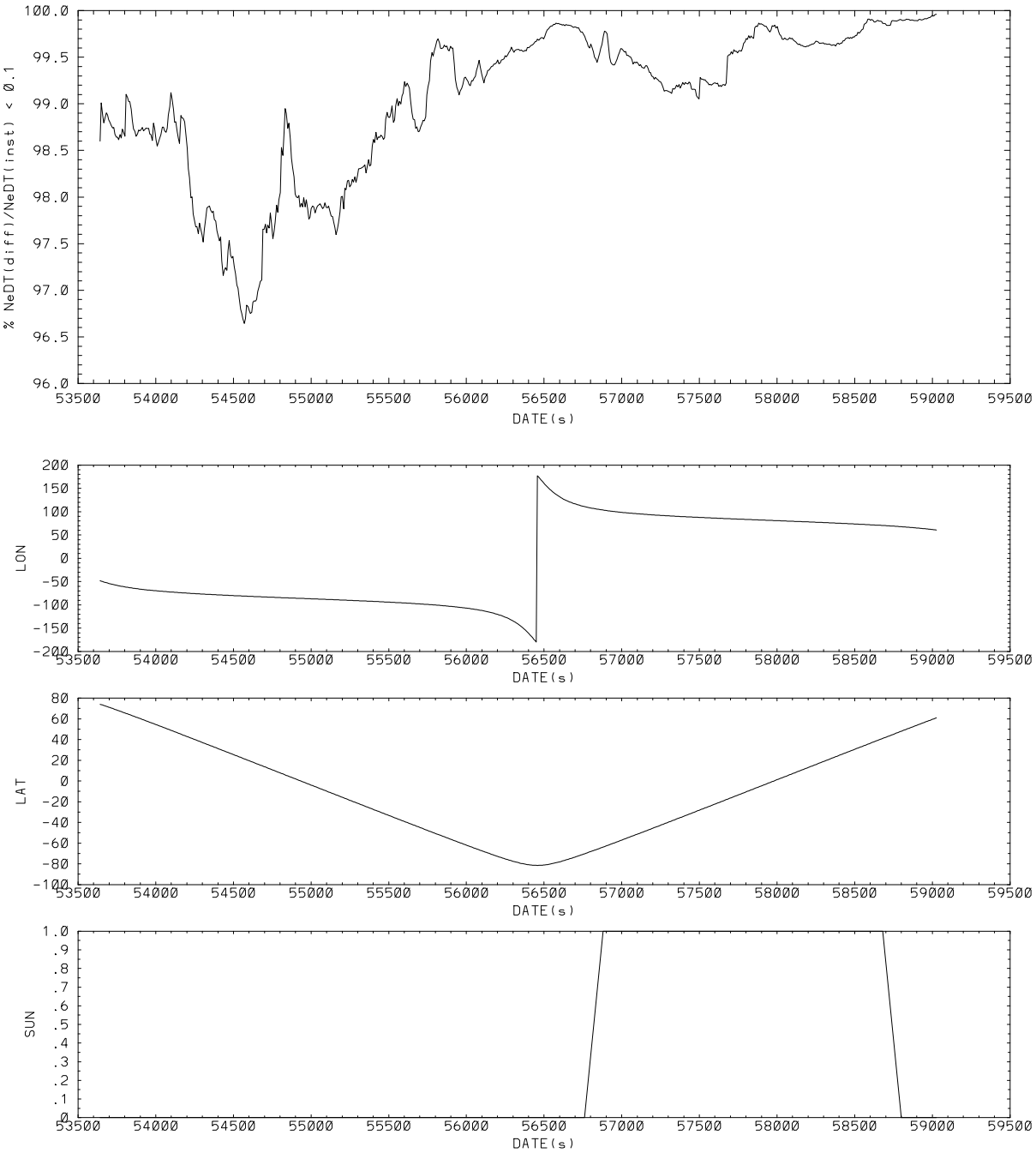

Figure 3: Comparison of IASI 1C spectra between local and global processing; number of cases where $NeDT(\Delta R) < 0.1 \times NeDT(inst)$; longitude; latitude; exposure to sun. X axis is second of the day.

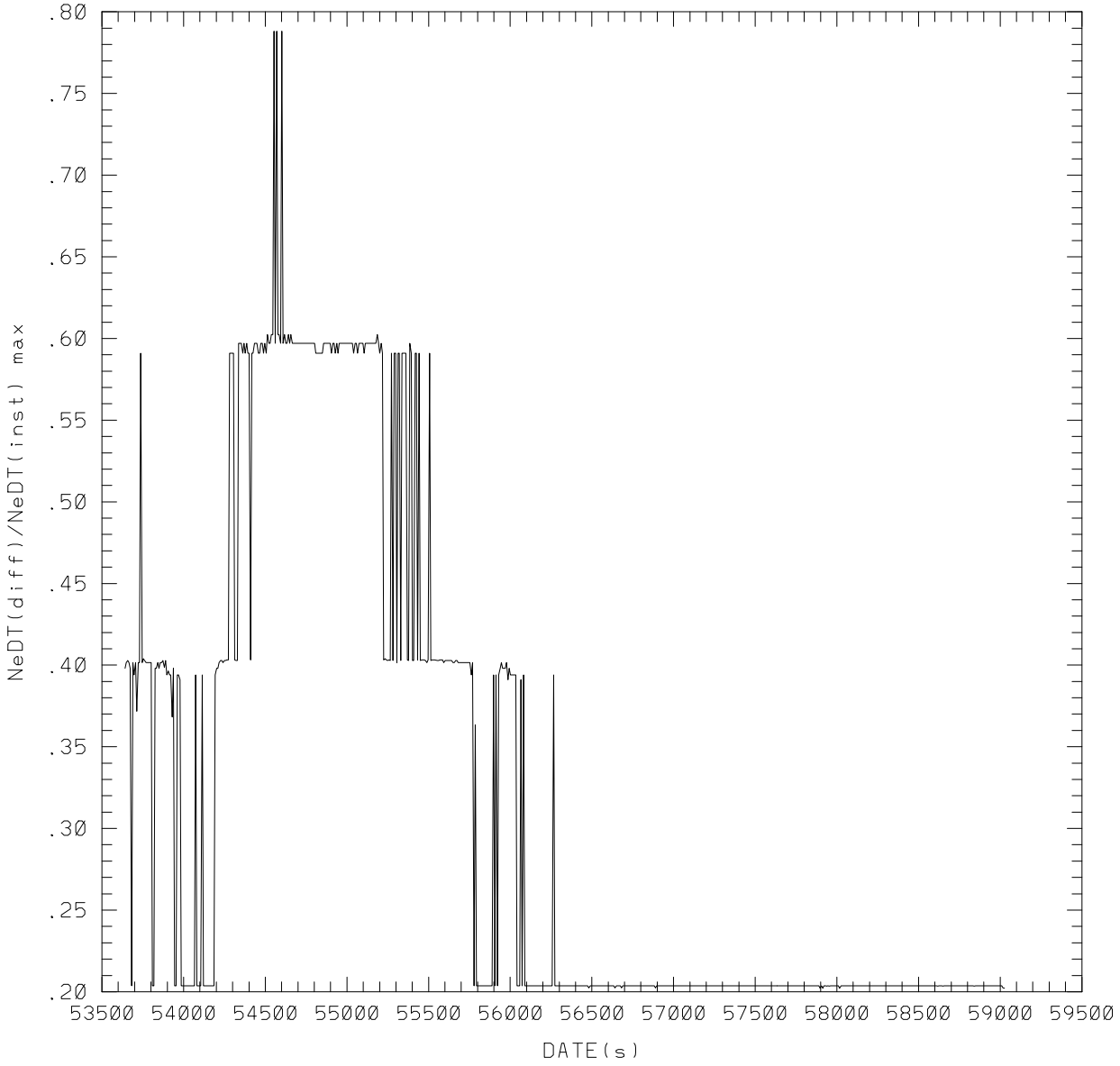

Figure 4: Maximum of $NeDT(\Delta R)/NeDT(inst)$ 1C spectra; for each scan line the maximum value is chosen, regardless of its wavenumber

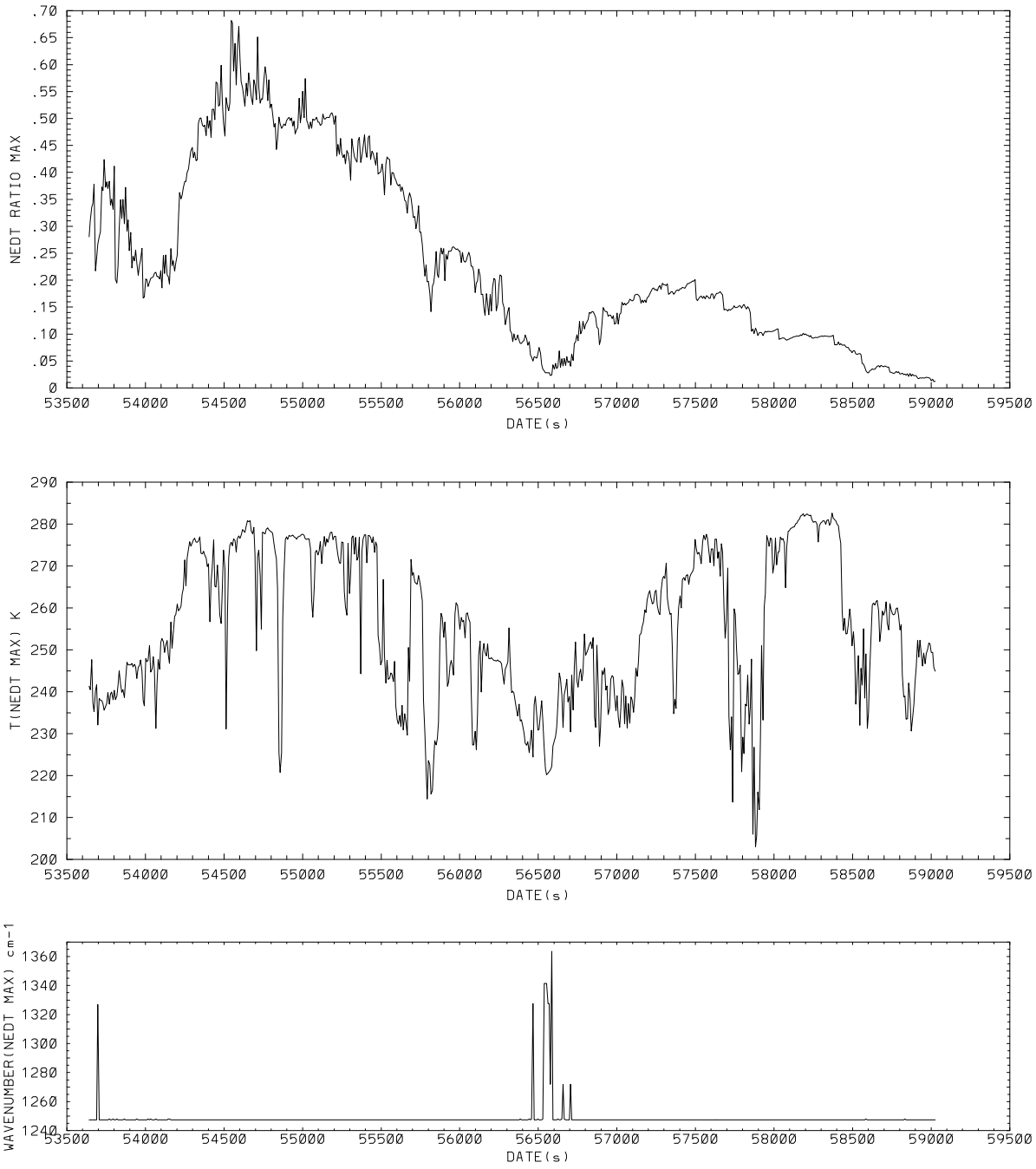

Figure 5: Maximum of $NeDT(\Delta R)/NeDT(inst)$ (non-discretized 1C spectra, double precision); associated brightness temperature; associated wavenumber.

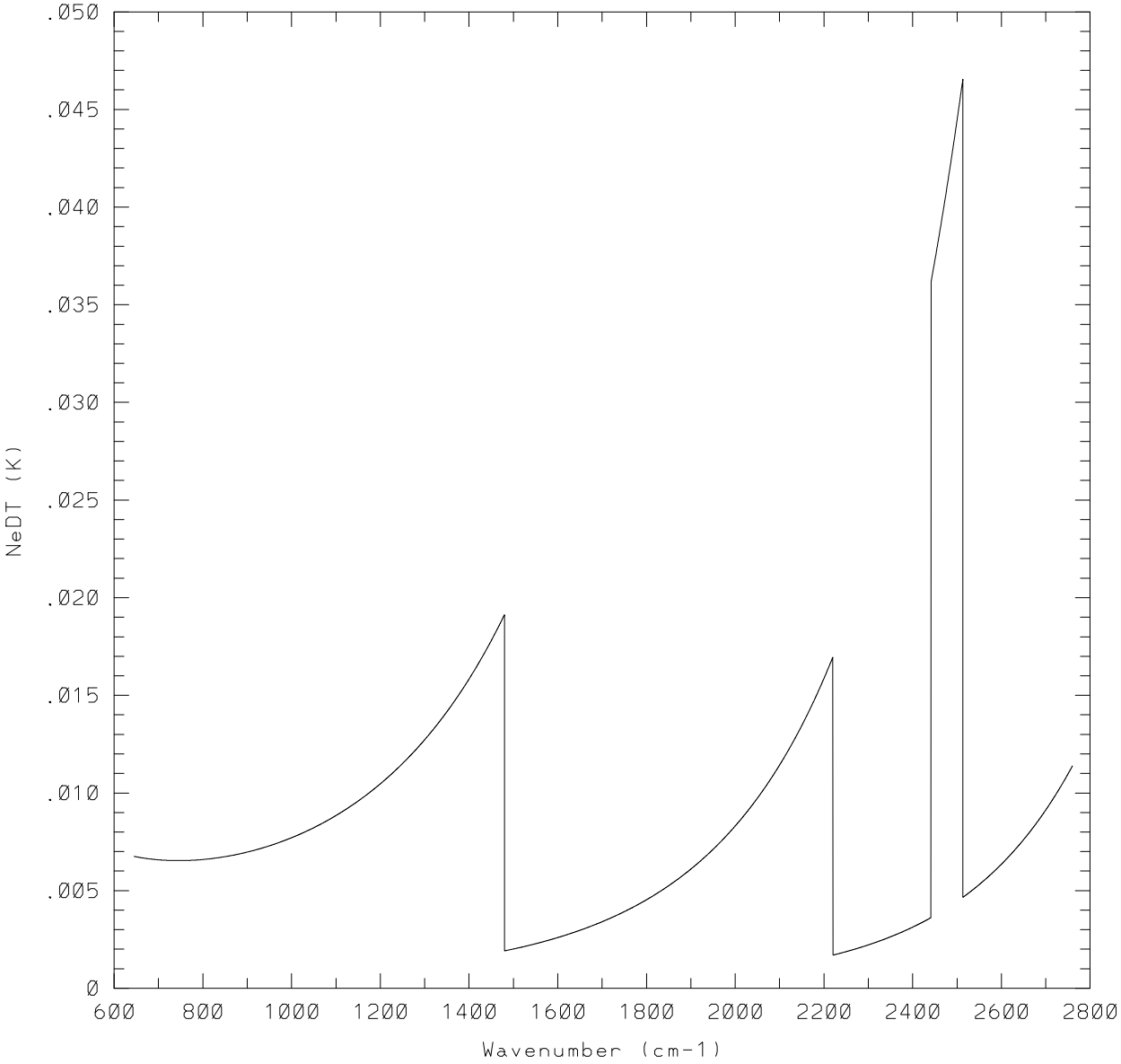

Figure 6: Variation of NeDT for a unit variation in numerical counts; with 1c scaling factors as of May 2007

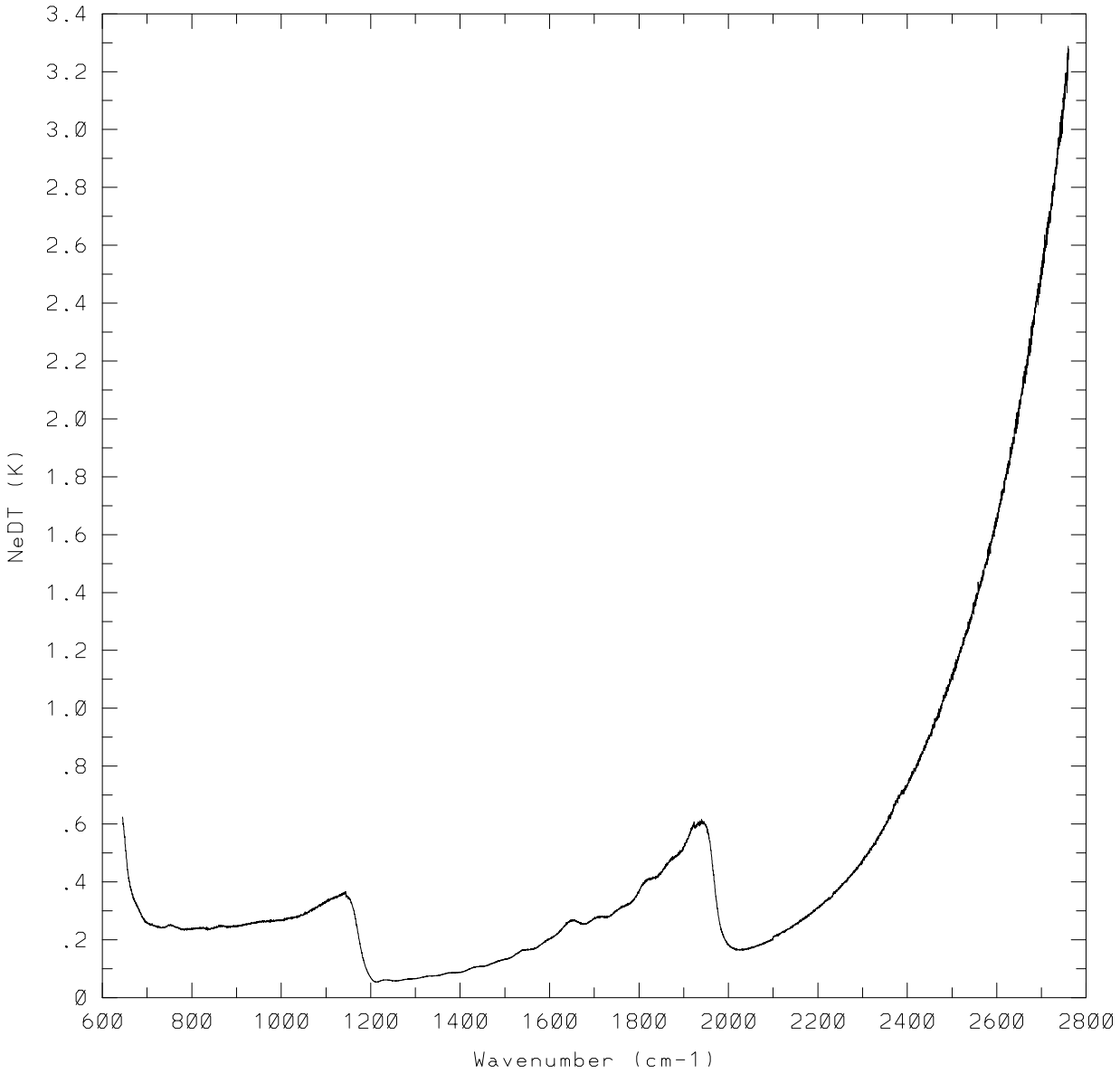

Figure 7: NeDT of IASI instrument; as provided by D. Blumstein (ISSWG18), NeDT IPR2 FM2 full resolution as of 30/11/2005

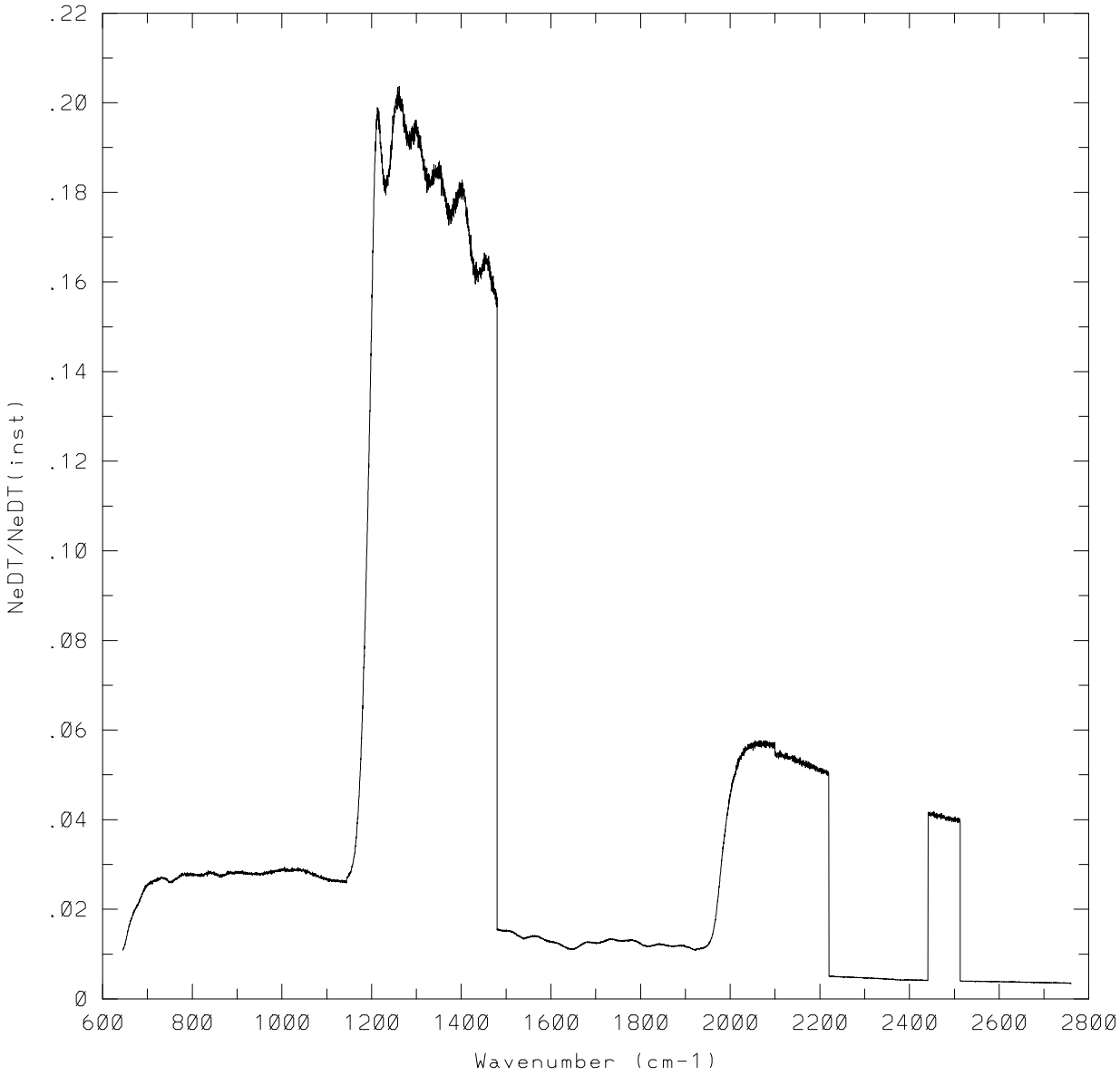

Figure 8: NeDT/NeDT(instr) for a unit variation in numerical counts

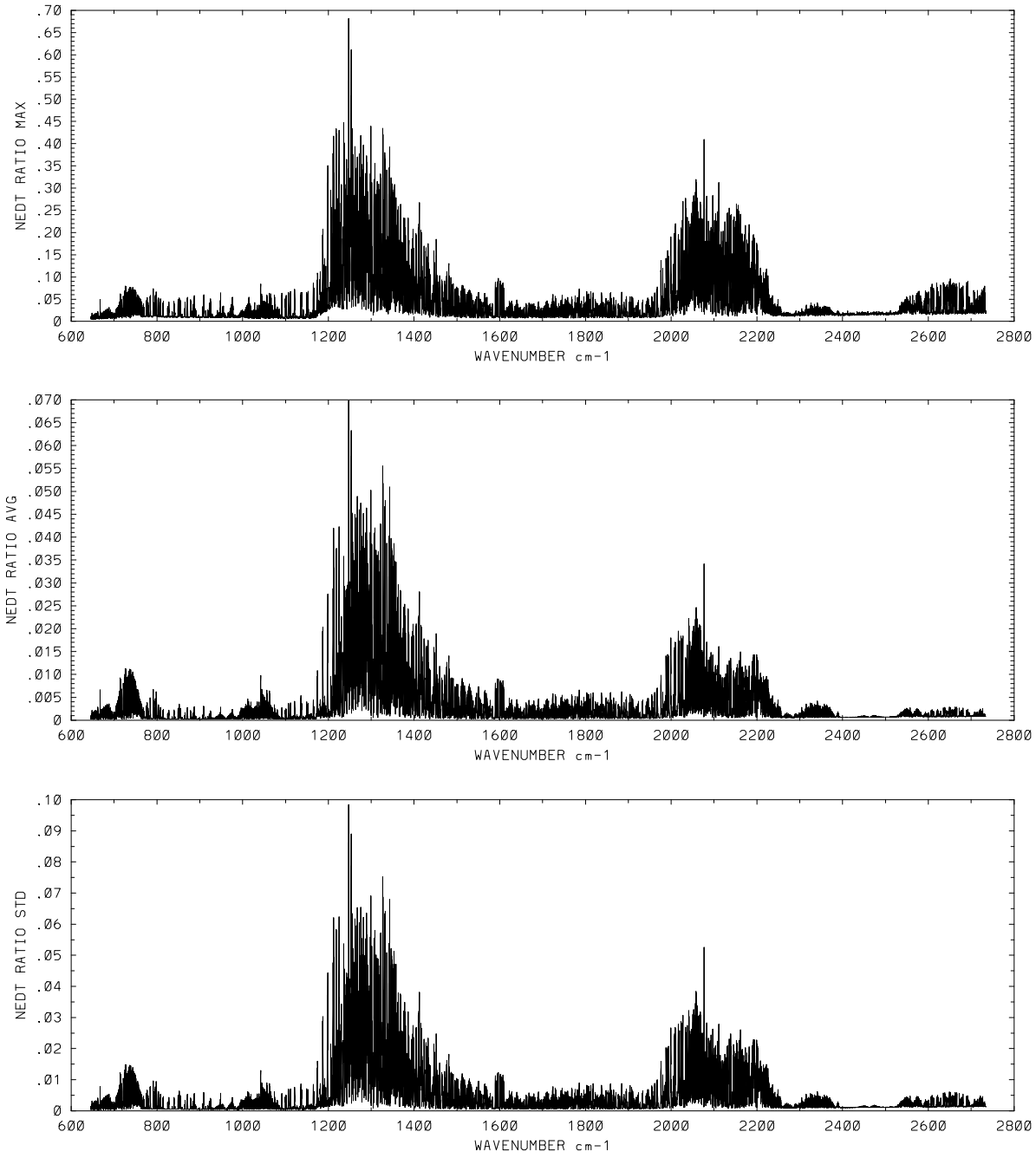

Figure 9: Maximum of NeDT(difference)/NeDT(instrument) (non-discretized spectra)

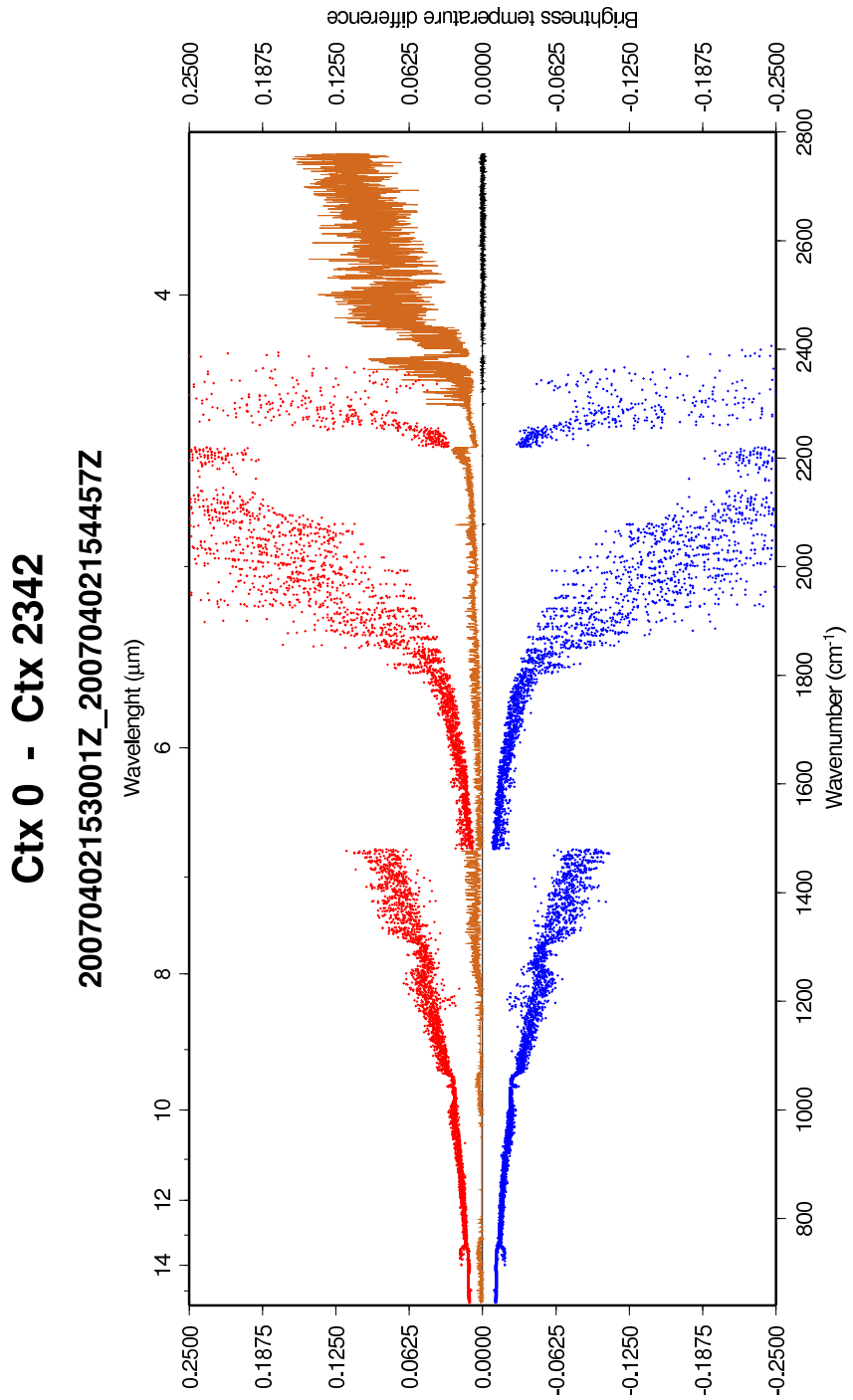

Figure 10: Brightness temperatures differences from time 55800 to 56700, orbit 2343, 15 minute period starting 30 minutes after start of processing

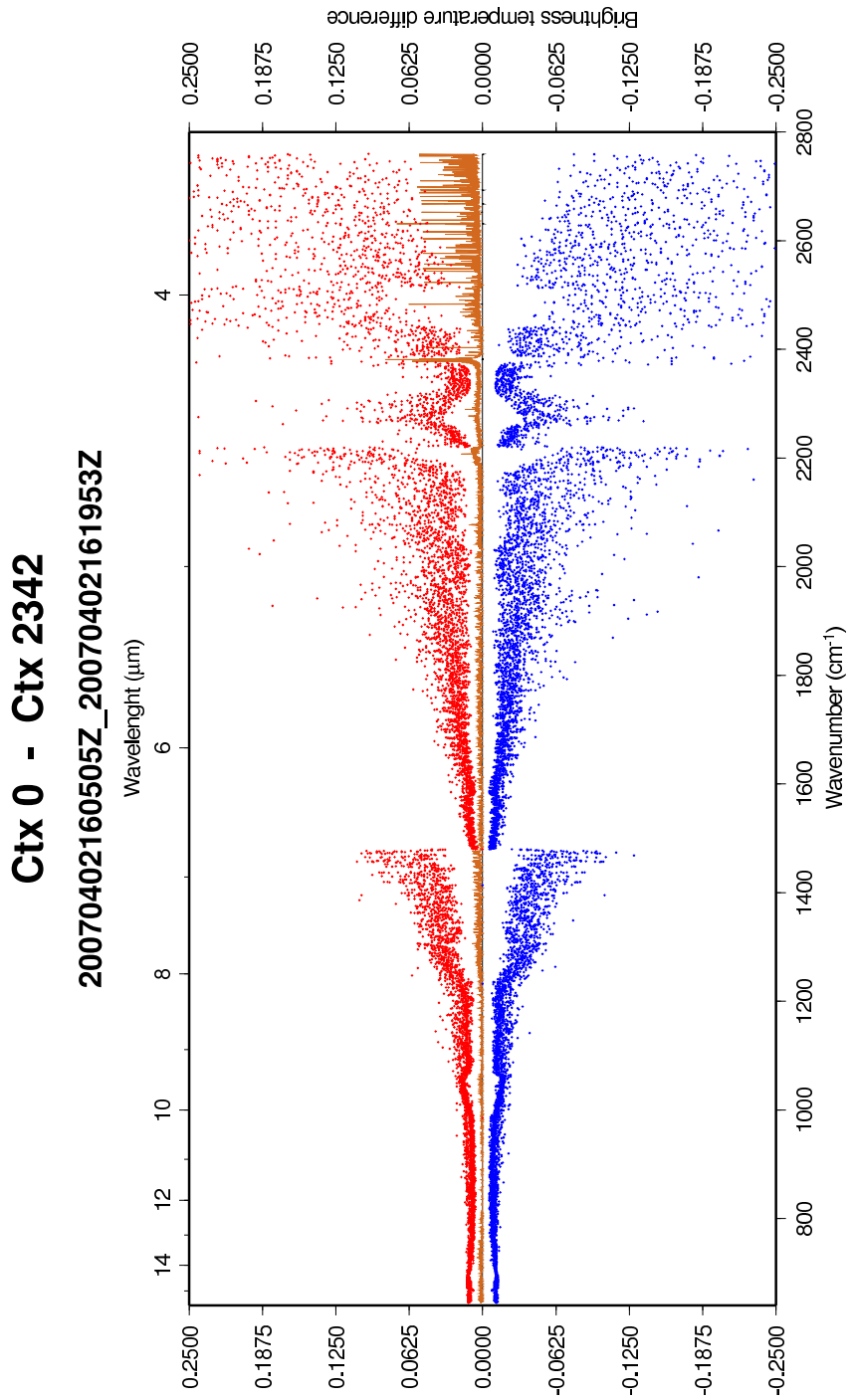

Figure 11: Brightness temperatures differences from time 57900 to 58800, orbit 2343, 15 minute period starting 70 minutes after start of processing

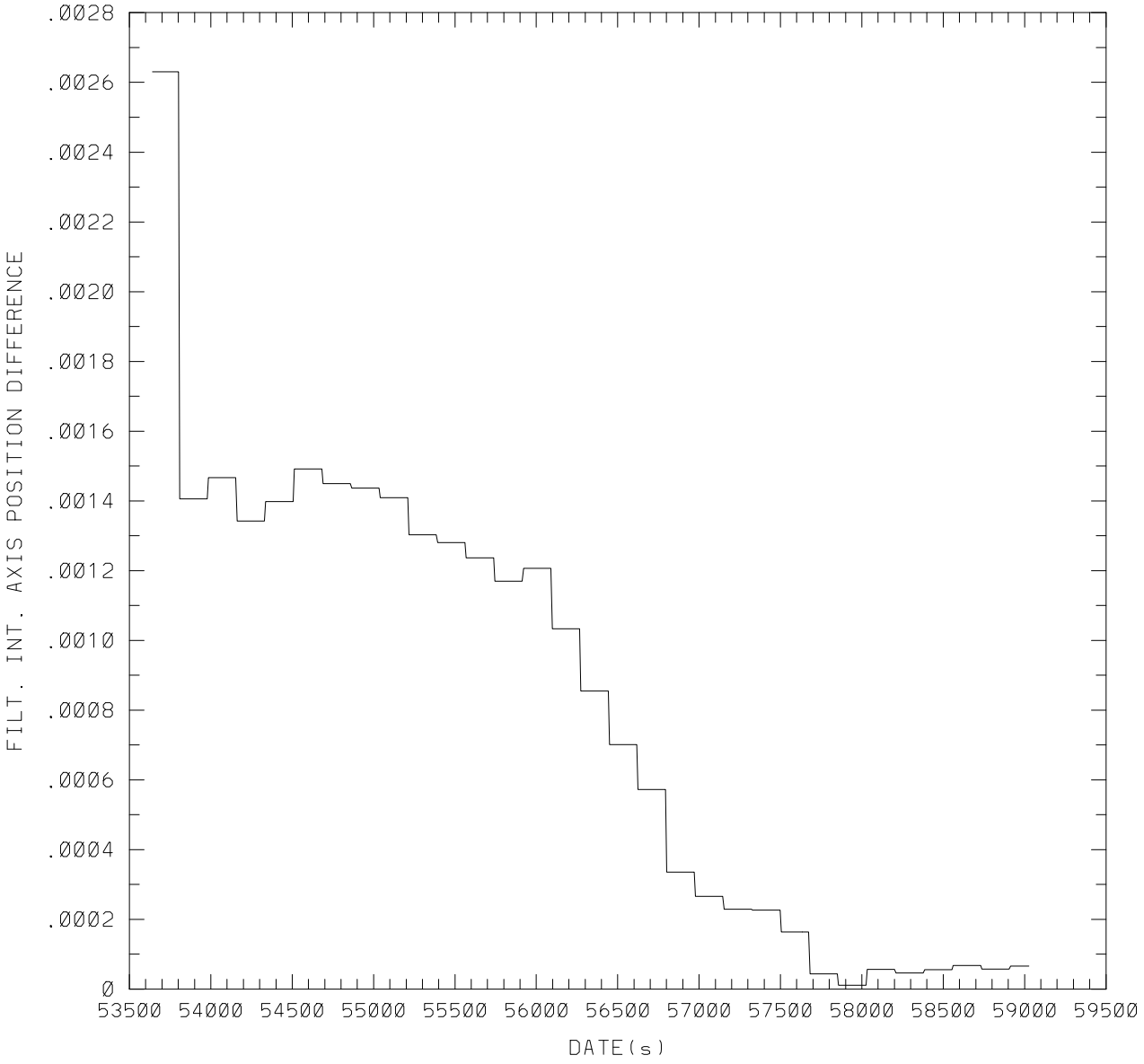

Figure 12: Difference (degrees) of filtered interferometer axis position, empty context, context 2342

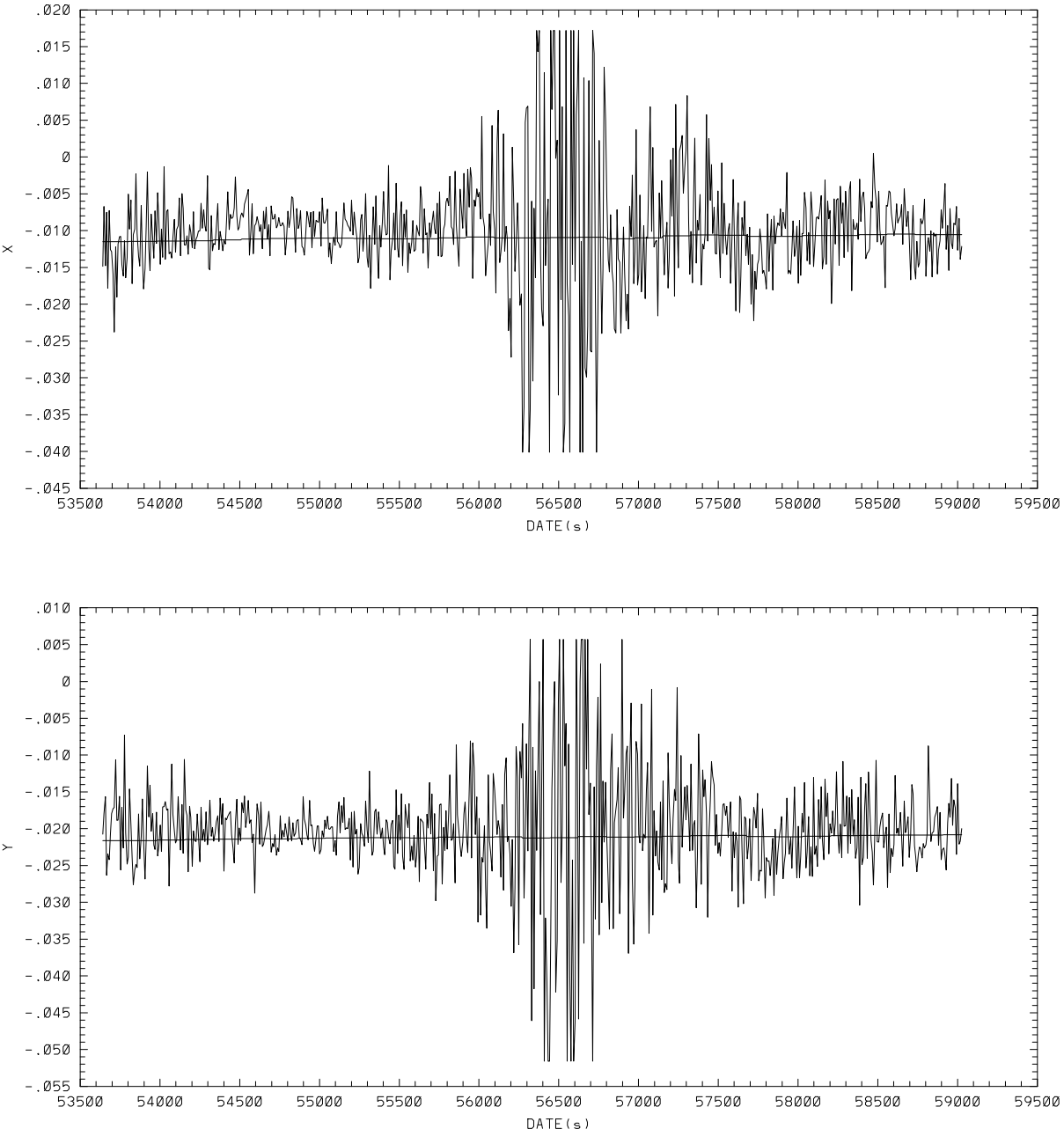

Figure 13: Position of interferometer axis position, instantaneous and filtered, starting from context 2342, GIaxAxeY, GFaxAxeY, GIaxAxeZ, GFaxAxeZ

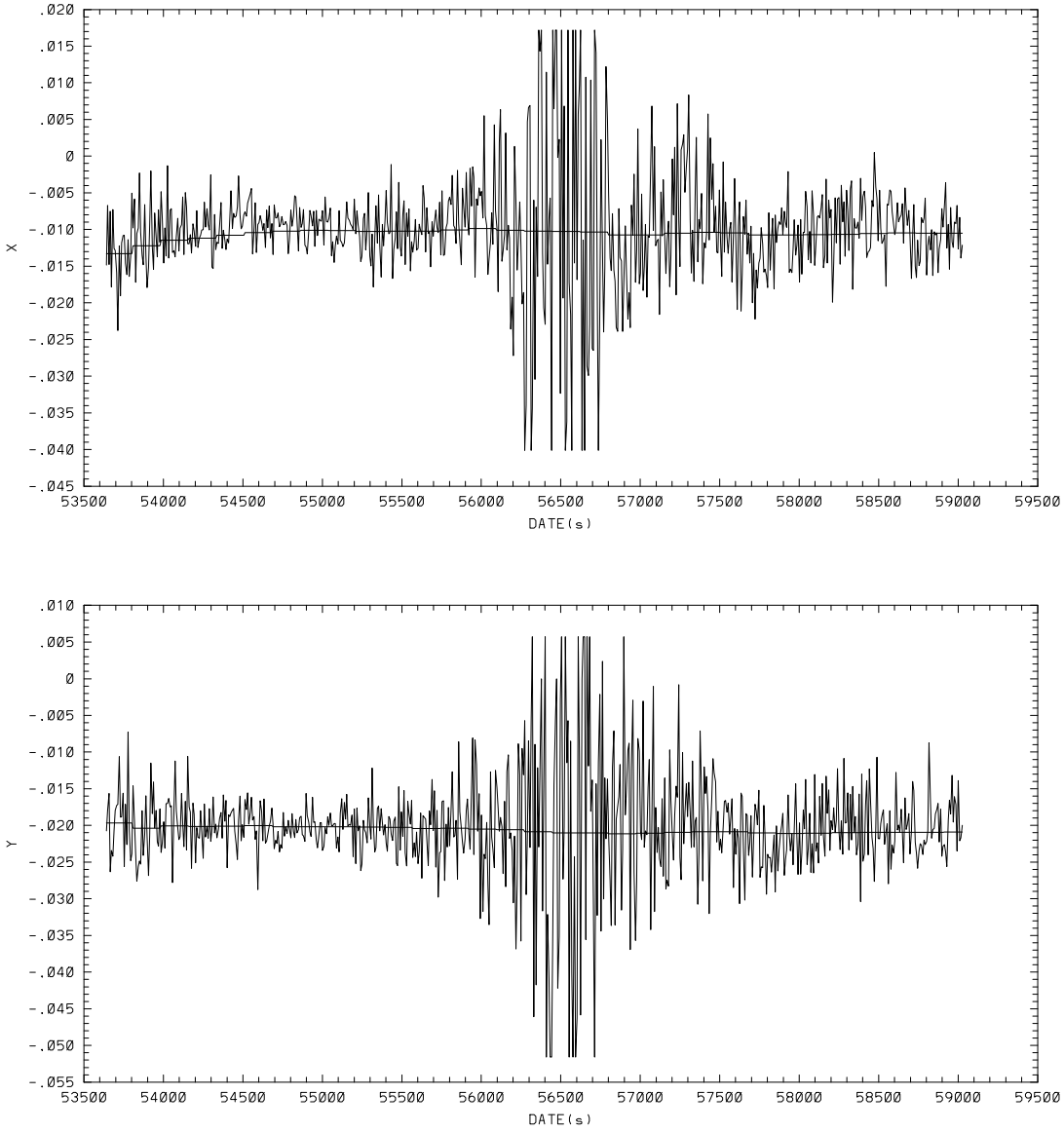

Figure 14: Position of interferometer axis position, instantaneous and filtered, starting from an empty context, GIaxAxeY, GFaxAxeY, GIaxAxeZ, GFaxAxeZ

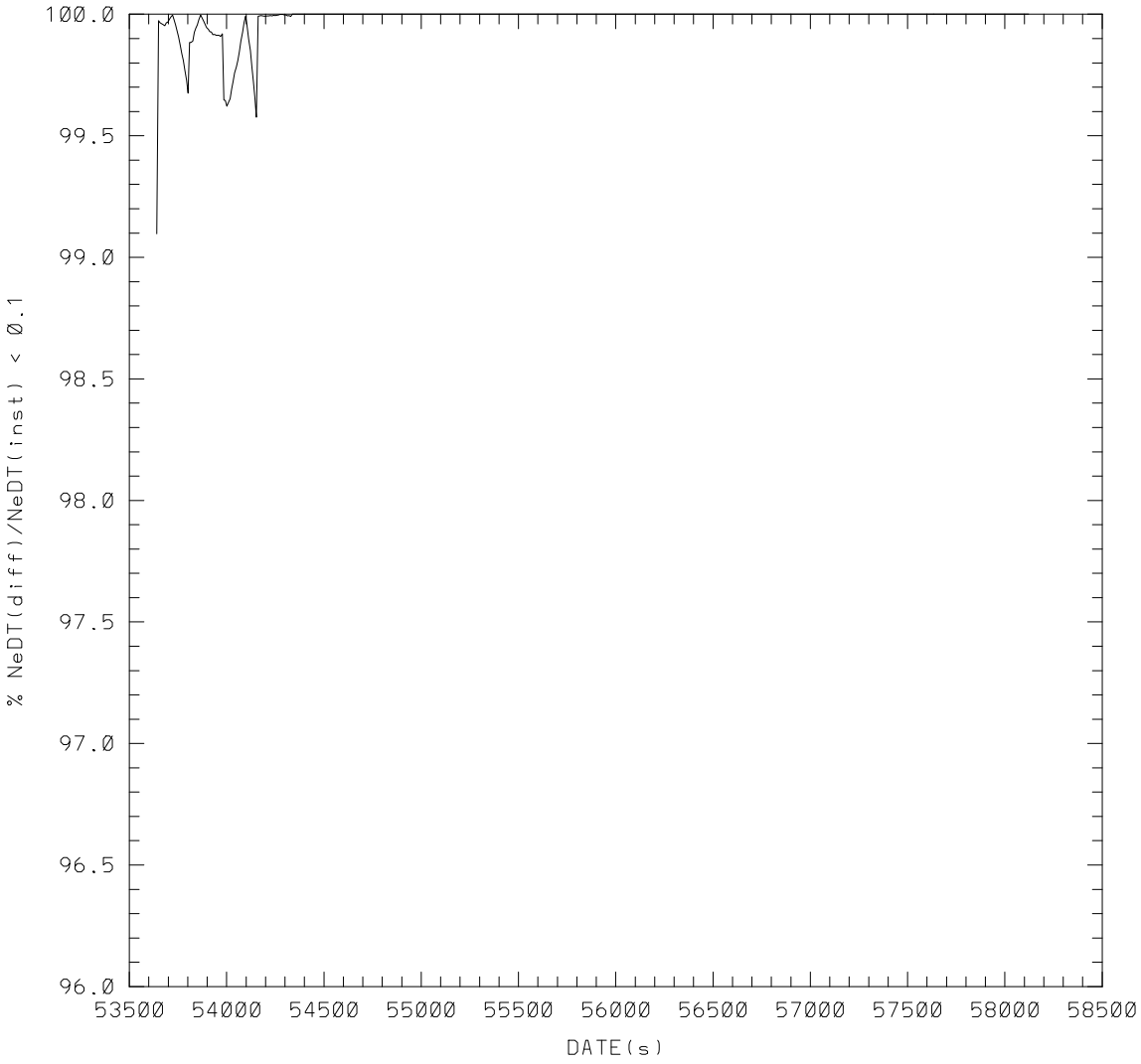

Figure 15: Comparison of IASI 1C spectra between global and local processing (non-empty axis position history)

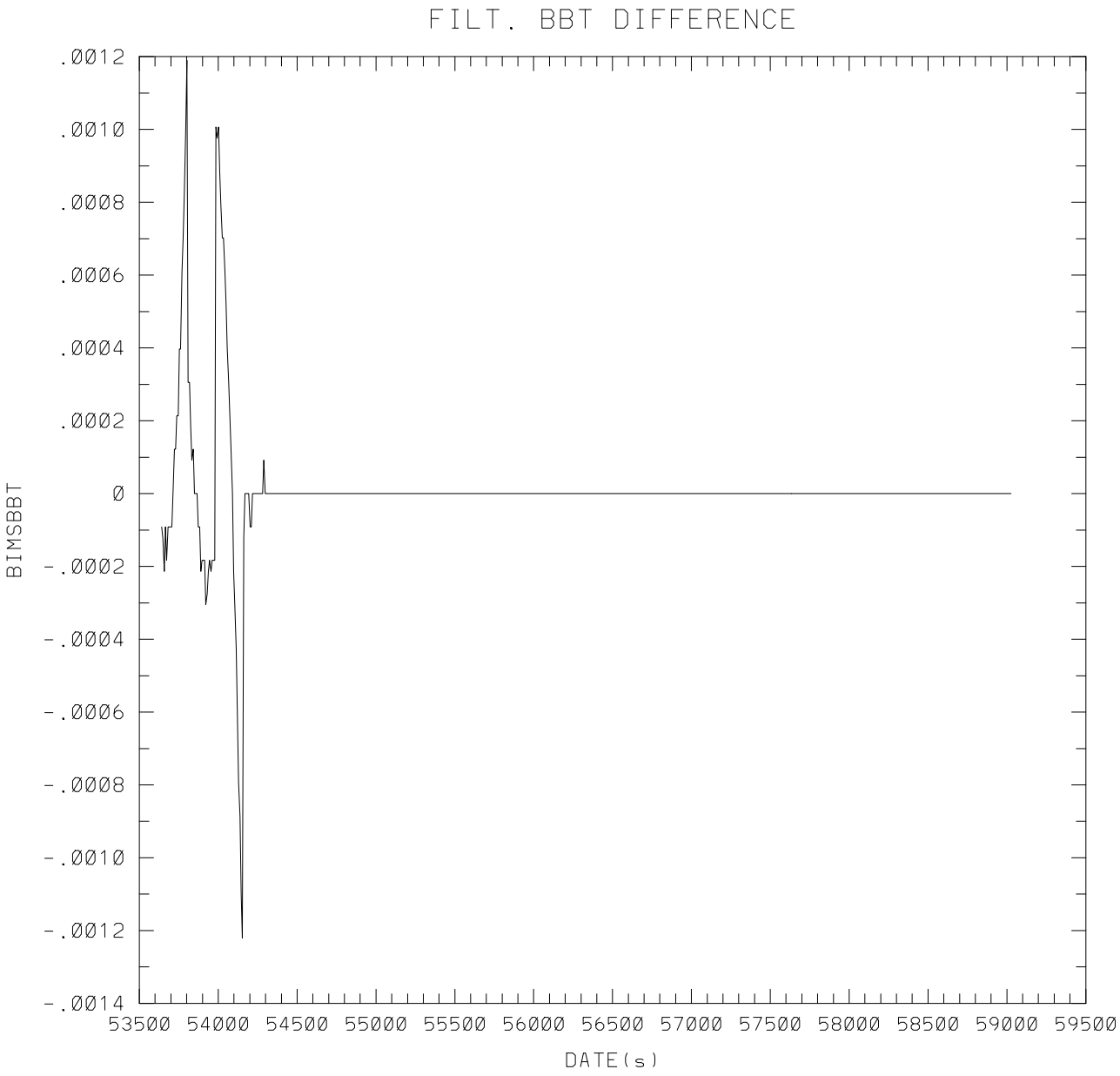

Figure 16: Difference of black body temperatures between runs based on empty context and context 2342

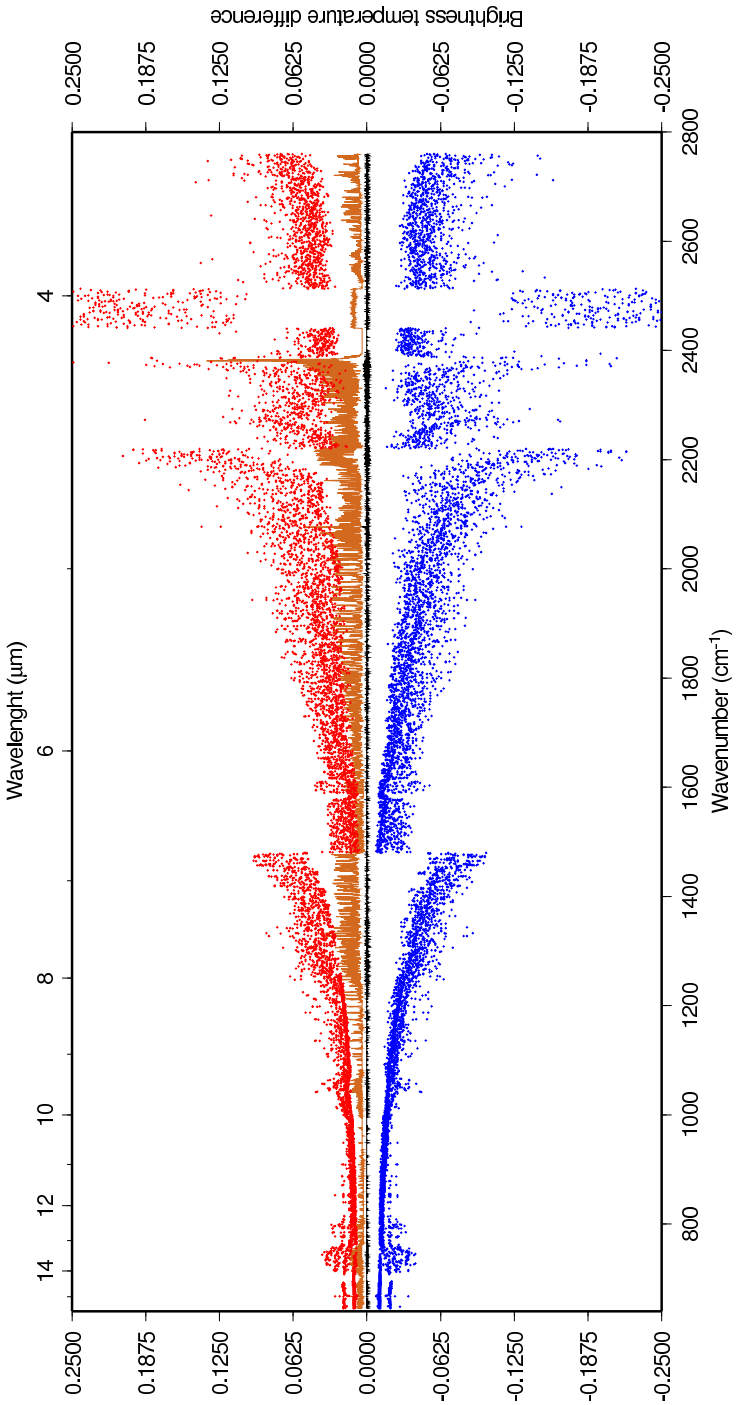

Figure 17: Differences of brightness temperatures between local and global processing 09:23 10/06/2007

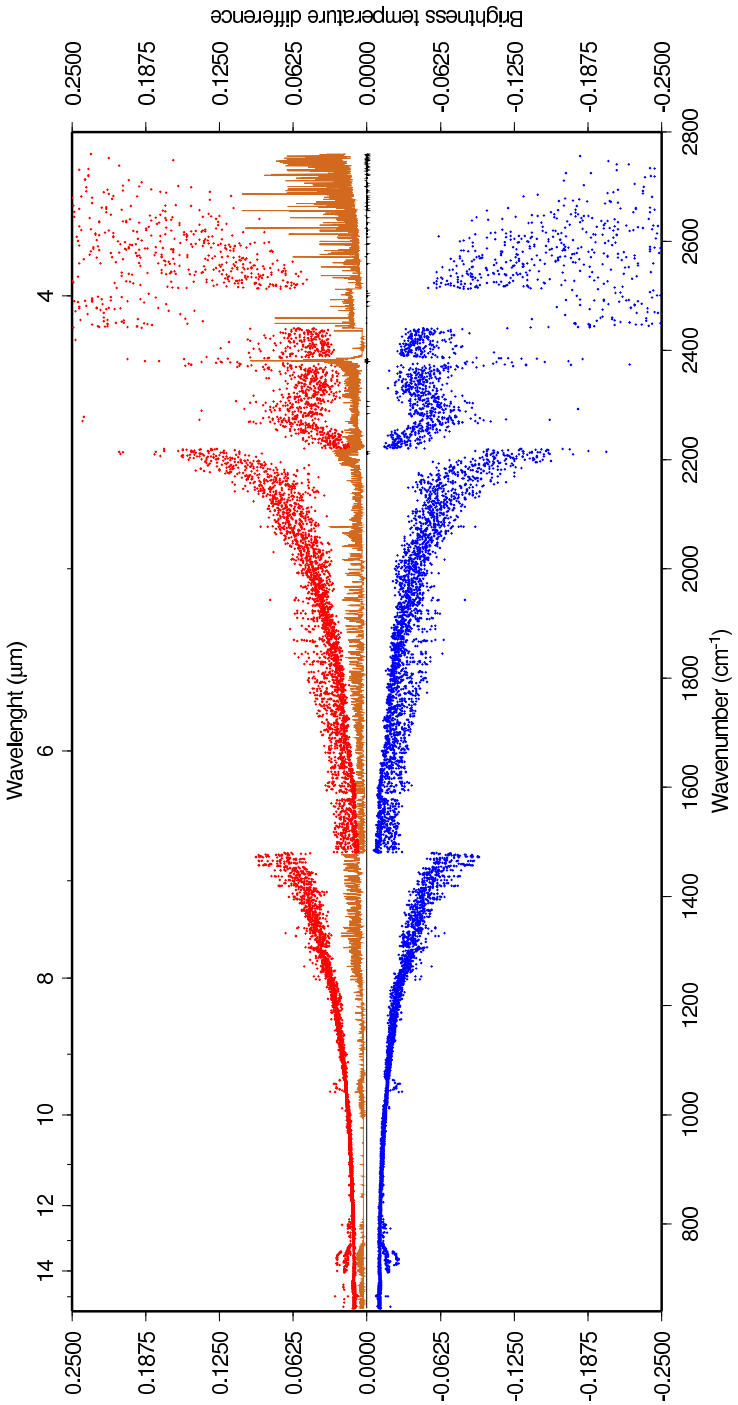

Figure 18: Differences of brightness temperatures between local and global processing 22:31 10/06/2007

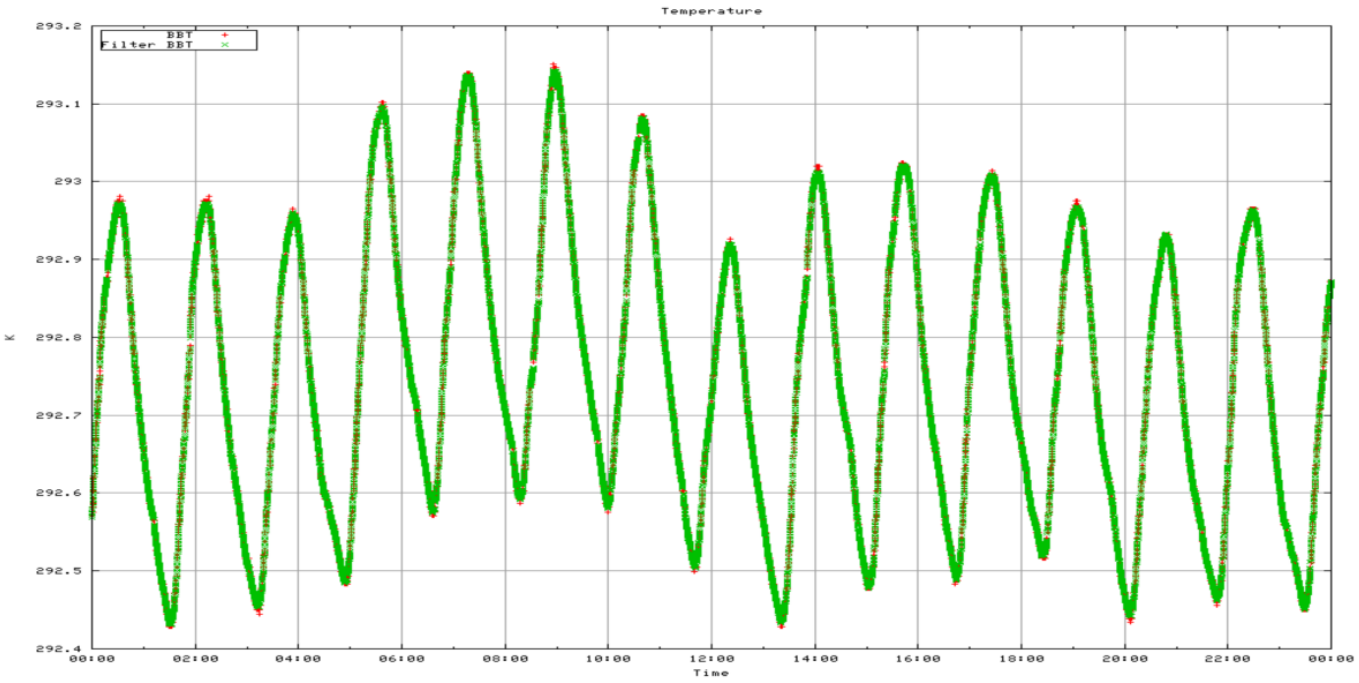

Figure 19: Variation of black body temperature over a one-day period 2007/06/03 (from L. Fiedler)

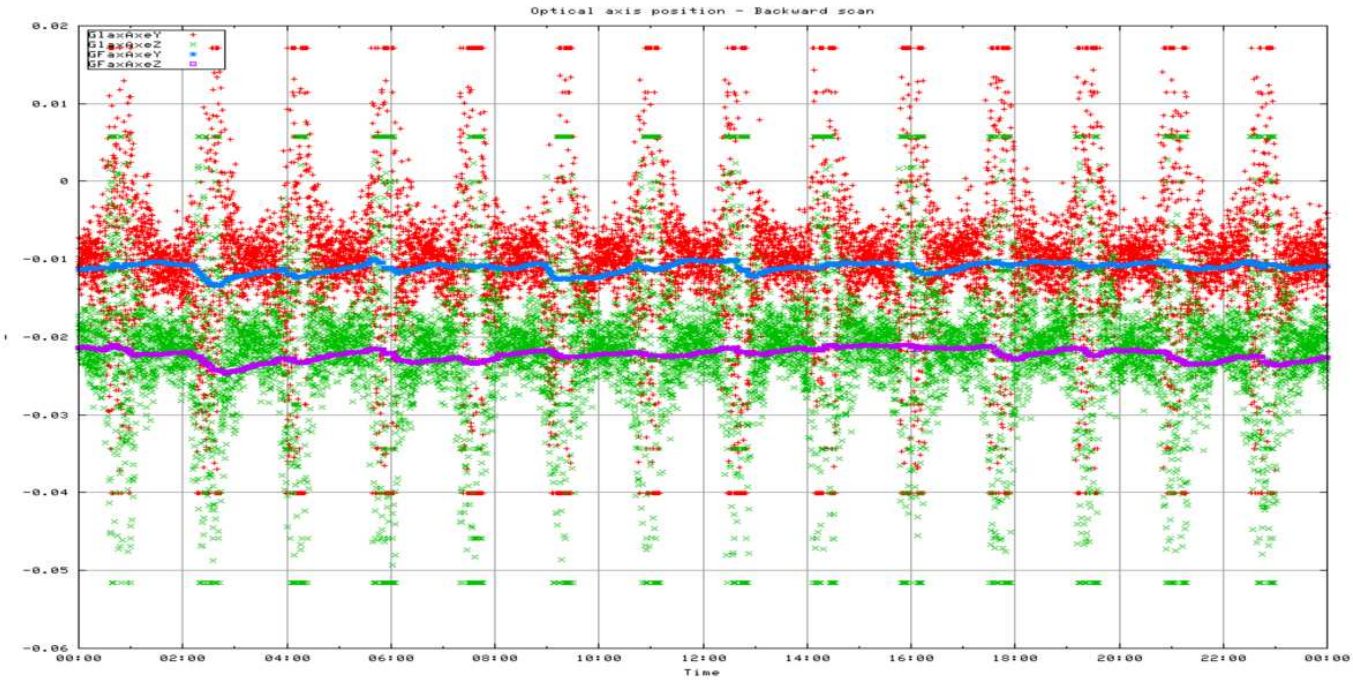

Figure 20: Evolution of interferometer axis position over a one-day period 2007/06/03 (from L. Fiedler)